Electronic Supplementary Material (ESI) for Physical Chemistry Chemical Physics.

Supporting Information

Dynamics of Nucleophilic Substitution on Ambident Nucleophile CN^- and Iodomethane: Insights into the Competition Mechanism with Neutral Isomeric Products

Xu Liu,[a] Shiqi Tian,[a] Boxue Pang,*[,b] Hui Li,[a] Yang Wu,*[,a]

[a]College of Chemistry, Liaoning University, Shenyang 110036, P. R. China

E-mail: liuxu@lnu.edu.cn, wuyang@lnu.edu.cn

[b]Key Laboratory of Ministry of Education on Safe Mining of Deep Metal Mines, School of Resources and Civil Engineering, Northeastern University, Shenyang, 110819, China

E-mail: pangboxue@126.com

Table S1. Electronic structure theory energies for stationary points of the S_N2 pathways on the $CN^- + CH_3I$ PES with different methods.[a]

Species	Method							
	MP2	B3LYP	B97-1	M06	M06-2X	BP86	MPW1K	CCSD(T)-F12b/PPQ[b]
XRC	-10.4	-9.9	-11.9	-13.1	-11.1	-13.6	-9.9	-10.2
XTS	-0.3	0.9	0.1	-0.8	-0.2	0.8	0.88	
RC1	-10.2	-9.3	-10.0	-9.91	-12.0	-10.12	-9.6	-9.7
RCTS	-10.1	-9.2	-9.8	-9.86	-9.5	-10.09	-9.4	-9.7
RC2	-10.7	-10.1	-10.7	-10.9	-11.1		-9.9	-10.2
TS1	-6.1	-8.9	-9.4	-7.8	-7.7		-7.0	-6.3
TS2	41.2	32.3	32.5	33.3	36.2	26.3	38.7	37.7
PC	-60.5	-60.9	-61.1	-61.2	-63.2	-61.0	-65.9	-60.6
XRC'	-9.6	-8.3	-9.9	-11.7	-9.9	-10.5	-8.4	-8.8
XTS'	-0.5	0.9	0.1	-0.7	-0.3	0.9	0.87	
RC1'	-10.6	-9.74	-10.33	-10.4		-10.11	-10.1	
RCTS'		-9.67	-10.30	-10.4	-10.1	-10.04	-9.8	
RC2'	-11.0	-10.0	-10.6	-11.2	-11.4	-10.7	-10.1	
TS1'	-2.0	-5.7	-5.8	-4.5	-4.2	-8.4	-3.7	-2.3
TS2'	45.9	36.0	36.6	36.9	40.6	30.6	43.0	42.6
PC'	-35.1	-38.2	-38.9	-38.5	-42.0	-37.3	-42.6	-36.6
P $NCCH_3 + I^-$	-48.1	-50.6	-49.8	-49.5	-51.1	-50.4	-55.1	-48.8
P' $CNCH_3 + I^-$	-21.4	-27.8	-27.4	-27.1	-29.5	-26.6	-31.8	-24.2

[a] Energies (in kcal/mol) are with respect to the $CN^- + CH_3I$ reactants and do not include ZPE.

[b] The higher level CCSD(T)-F12b/PPQ energy comes from reference: Z. Kerekes, D. A. Tasi and G. Czakó, J. Phys. Chem. A, 2022, 126, 889-900.

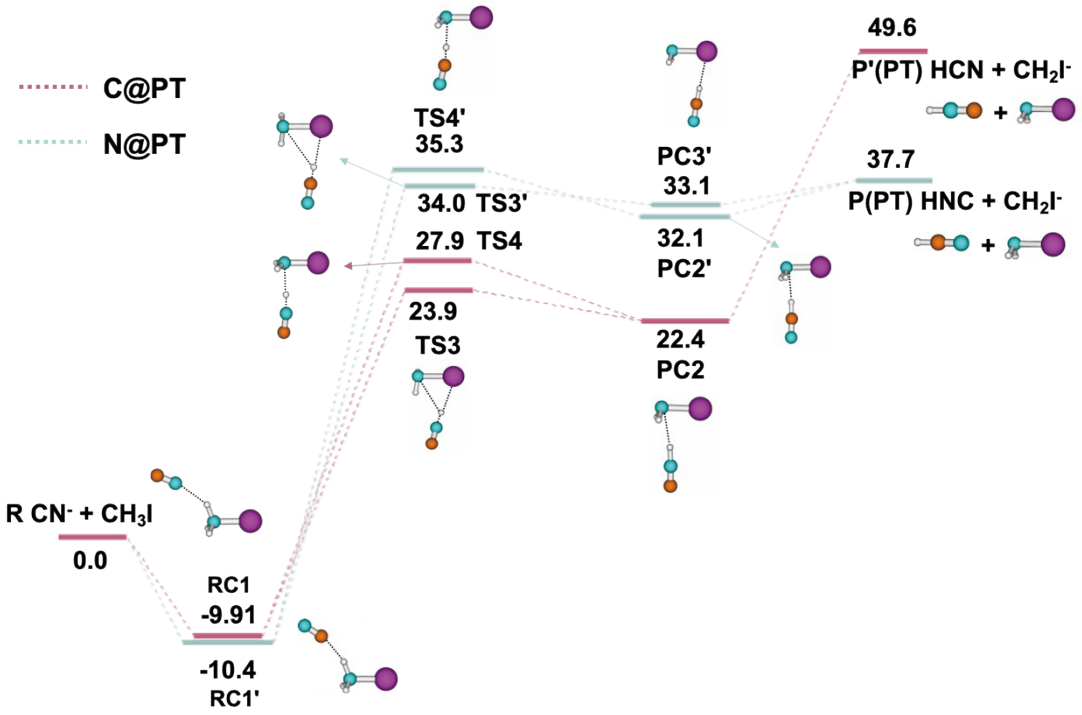

Figure S1. Potential energy profile and stationary points for proton transfer pathways in reaction CN^- + CH_3I at the M06/ECP/d level of theory. Energies in kcal/mol are relative to reactants without zero-point energy (ZPE).

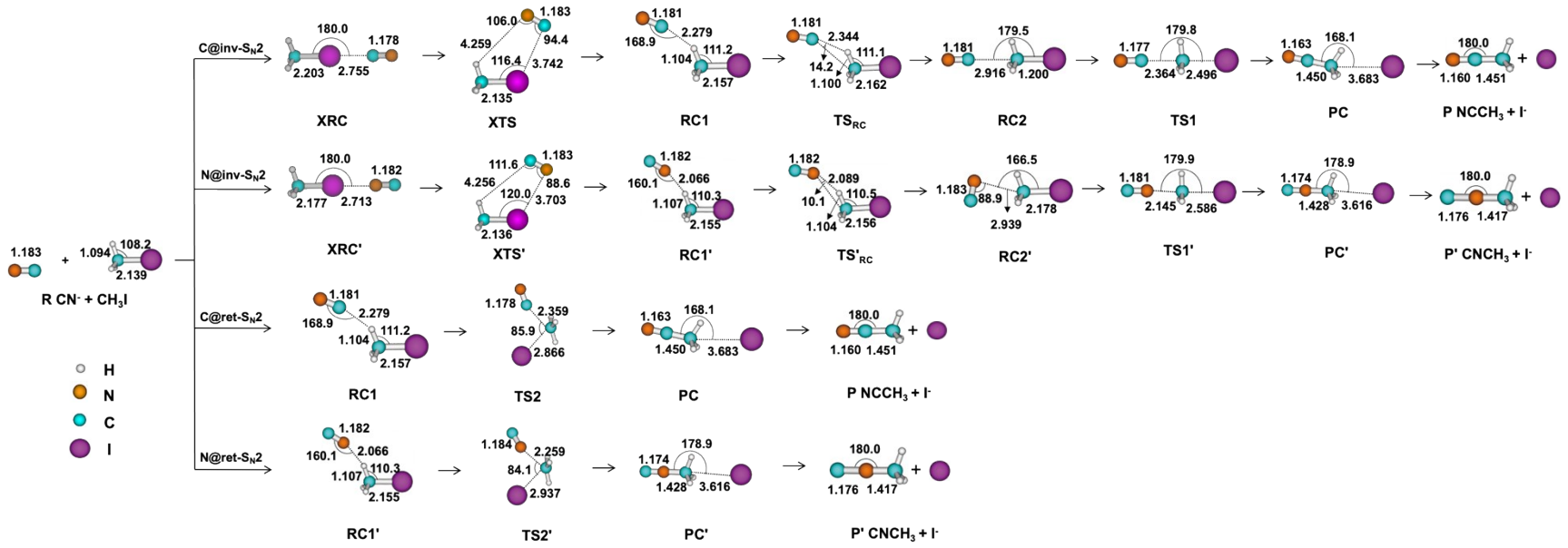

Figure S2. M06/ECP/d geometries of stationary points for S_N2 pathways in the CN^- + CH_3I reaction. Bond distances are in Å and angles in degree.

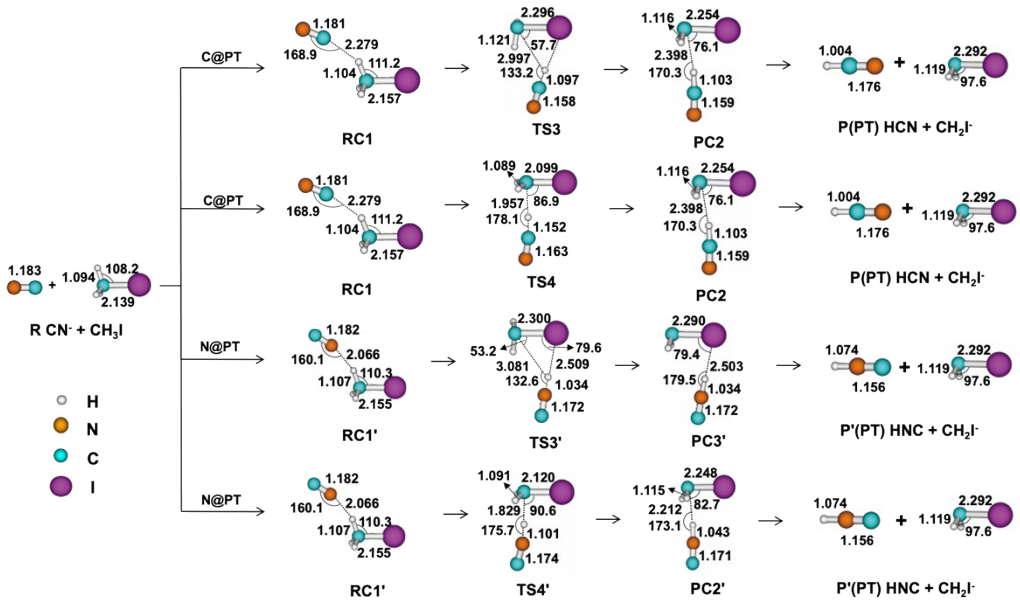

Figure S3. Stationary point structures of proton transfer channels in the CN^- + CH_3I reaction optimized at the M06/ECP/d level of theory. Bond distances (in Å) and angles (in degree).

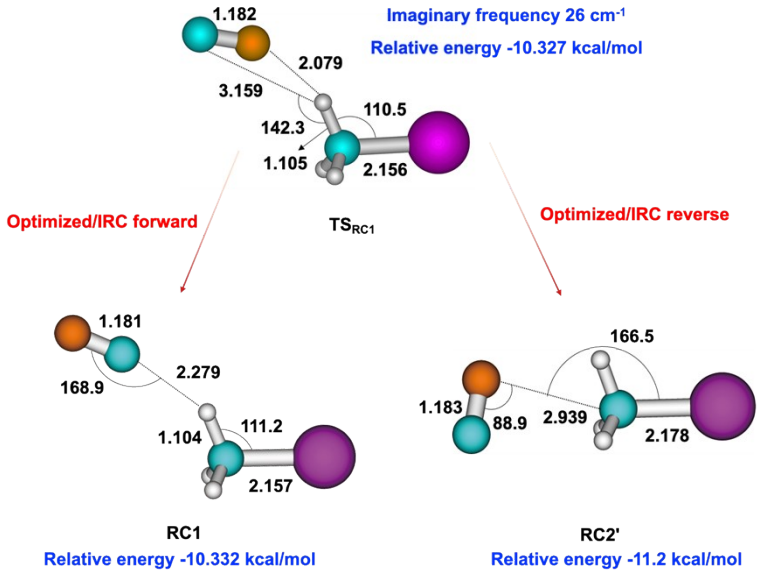

Figure S4. Geometries of transition state TS_{RC1} between RC1 and RC2' for the CN^- + CH_3I reaction optimized at the M06/ECP/d level of theory. Bond distances are in Å and angles are in degrees.

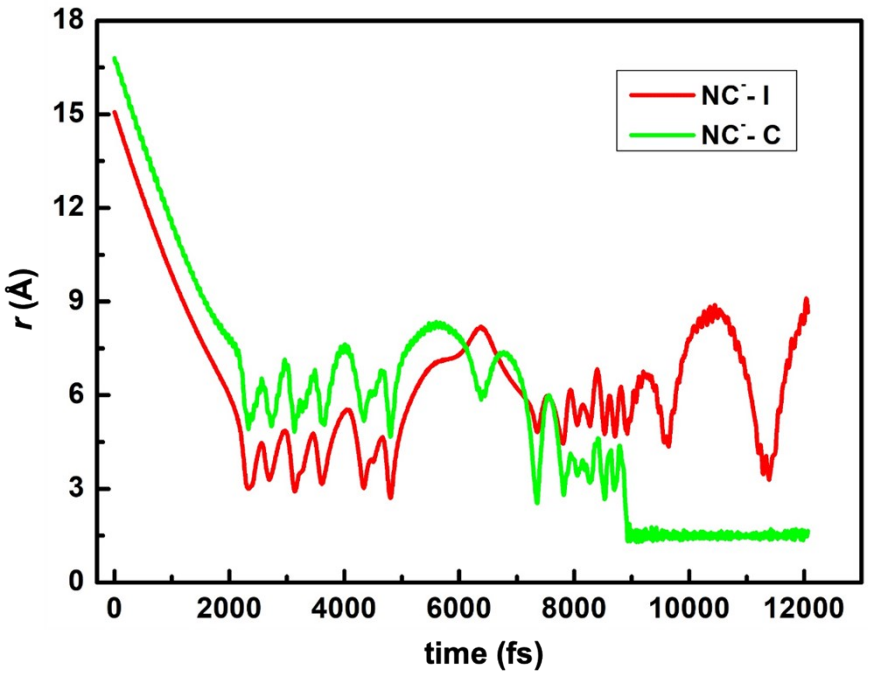

Figure S5. Representative plots of the distance (Å) between C of CN^- and C/I of CH_3I versus time (fs) with pre + halogen + post mechanism for $CN^- + CH_3I \rightarrow CH_3CN + I^-$ reaction.

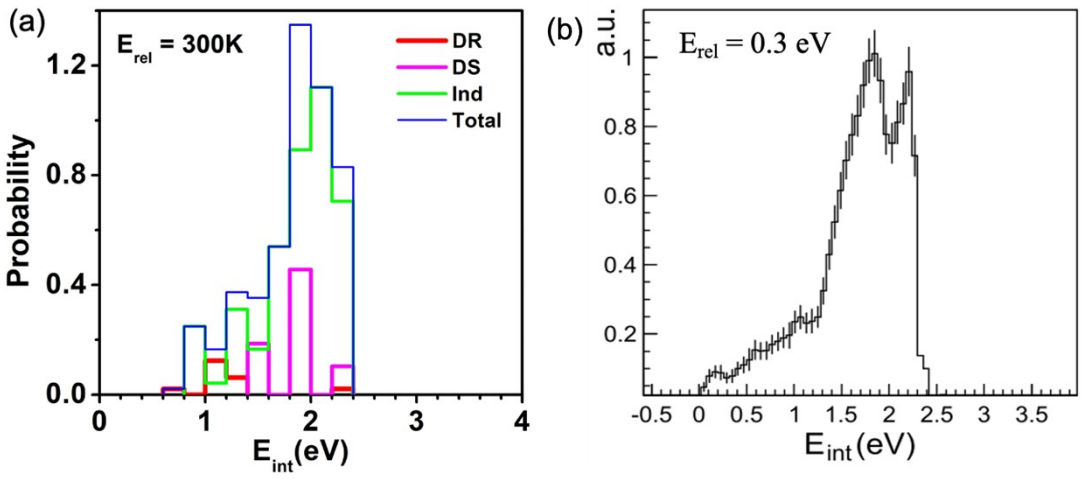

Figure S6. Product internal energy distributions from reactions of CN^- + CH_3I S_N2 reaction. (a) Products energy distributions at room temperature are illustrated for the direct rebound (red), direct stripping (light purple), and indirect (green) mechanisms and for the total scattering (dark blue). (b) The experimental energy distributions at low collision energy 0.3 eV in ref. E. Carrascosa, M. Bawart, M. Stei, F. Linden, F. Carelli, J. Meyer, W. D. Geppert, F. A. Gianturco and R. Wester, *J. Chem. Phys.*, 2015, **143**, 184309.

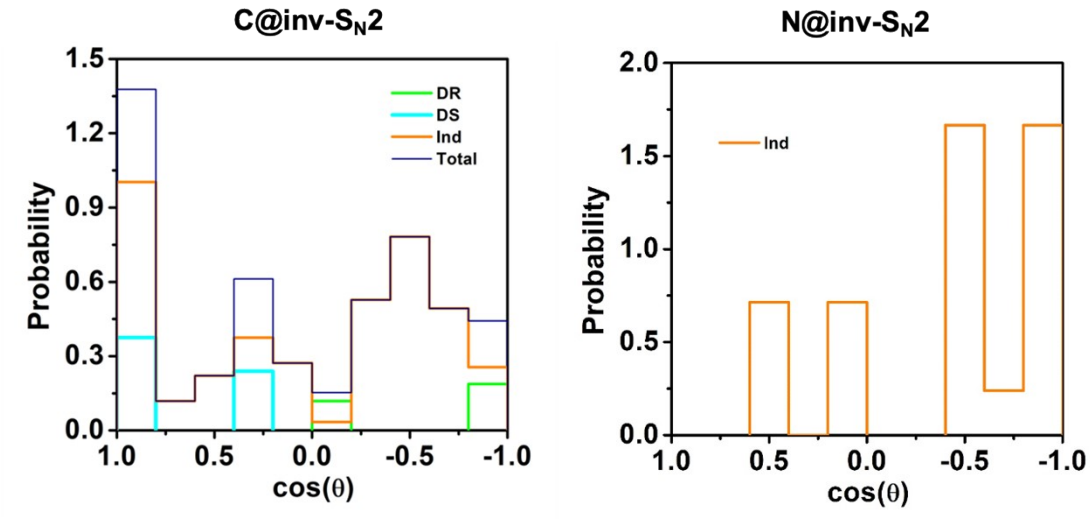

Figure S7. Velocity scattering angle distributions for the individual reaction mechanisms and for the C@inv-S_N2 and N@inv-S_N2 reaction channels. The green, light blue, orange, and dark blue lines represent the direct rebound, direct stripping, indirect reactions, and total reaction, respectively. The trajectory results are properly weighted by *b* and the reaction probability versus *b*.

Animations S1 - S8

Animation S1. A trajectory following the direct rebound (DR) mechanism for the C@inv-S_N2 reaction $CN^- + CH_3I \rightarrow CH_3CN + I^-$.

Animation S2. A trajectory following the direct stripping (DS) mechanism for the C@inv-S_N2 reaction $CN^- + CH_3I \rightarrow CH_3CN + I^-$.

Animation S3. A typical indirect trajectory trapped in pre-reaction potential energy well and forming reaction intermediates RC1/RC1' and RC2/RC2' (see Figure 1) for the C@inv-S_N2 reaction.

Animation S4. A typical indirect trajectory trapped in pre-reaction potential energy well and forming reaction intermediates XRC/XRC', RC1/RC1' and RC2/RC2' (see Figure 1) for the C@inv-S_N2 reaction.

Animation S5. A typical indirect trajectory trapped in both pre-reaction and post-reaction potential energy wells and forming reaction intermediates RC1/RC1', RC2/RC2' and PC (see Figure 1) for the C@inv-S_N2 reaction.

Animation S6. A typical indirect trajectory trapped in both pre-reaction and post-reaction potential energy wells and forming reaction intermediates XRC/XRC', RC1/RC1', RC2/RC2' and PC (see Figure 1) for the C@inv-S_N2 reaction.

Animation S7. A typical indirect trajectory trapped in pre-reaction potential energy well and forming reaction intermediates RC1/RC1' and RC2/RC2' (see Figure 1) for the N@inv-S_N2 reaction $CN^- + CH_3I \rightarrow CH_3NC + I^-$.

Animation S8. A typical indirect trajectory trapped in both pre-reaction and post-reaction potential energy wells and forming reaction intermediates RC1/RC1'

RC2/RC2' and PC' (see Figure 1) for the N@inv-S_N2 reaction $CN^- + CH_3I \rightarrow CH_3NC + I^-$.